STATISTICAL DOWNSCALING OF EXTREME PRECIPITATION

P. Garrett[1], N. Grosso[1], L. F. Dias[1]
1 Climate Change Impacts, Adaptation & Modelling Research Group, Faculty of Sciences, University of Lisbon, Portugal

ABSTRACT

Climate change impacts are highly dependent on regional geographical features, local climate variability, and socio-economic conditions. Climate change Impact assessment studies should therefore be performed at the local or at most at the regional level for the evaluation of possible impacts. However, climate scenarios are produced by Global Circulation Models with spatial resolutions of several hundred kilometres. Downscaling methods are thus needed to bridge the gap between the large scale climate scenarios and the fine scale where local impacts happen.

The aim of this work was to assess the use of statistical downscaling methods to model precipitation extremes focusing on the urban areas of Lisbon and Coimbra. The overall results for Lisbon showed high uncertainties in the definition of signal trend. With the exception of the 2 years return period both scenarios diverge, with uncertainty increasing by the end of the XXI century and in higher return periods. Nevertheless, for 2050's both scenarios tend to agree on higher return periods when compared with the reference values. For Coimbra the results clearly show a convergence in both scenarios for a decrease in the return periods for the mid and end of the XXI century. With the exception of the 2 years return period all projection indicate that all return levels will likely become twice as frequent at the end of the century.

1 INTRODUCTION

Global Circulation Models (GCMs) are widely used to assess climate change at a global scale, i.e. the global warming. However, GCMs outputs, with a grid cell size with hundreds of kilometers in length, are not enough to assess the detailed changes at regional/local levels. In fact, most impact studies are done for spatial resolutions of the order of a few square kilometers and even lower in the case of regions of complex topography, coastal or island locations or with highly heterogeneous land-cover (Wilby, 2004).

In these cases it would be adequate to resort to Regional Climate Models (RCMs), with a spatial resolution of the order of tens of kilometers or even less. Nevertheless bridging the gap between the resolution of global climate models and local scale weather and microclimatic processes represents a considerable technical challenge.

RCMs derive from the application of dynamical downscaling methods. They take as domain boundary conditions the larger scale atmospheric and sea surface variables supplied by the global coupled Atmospheric and Ocean Global Circulation Models (AOGCMs), in a process called “nesting”, where RCM grid-boxes nest inside one or more GCM grid-boxes. Like GCMs, RCMs are based on numerical simulations of the physical processes operating in nature.

Unfortunately RCM still have several drawbacks, for example, they have limited number of available experiments/scenario runs and time periods. The main limitation is that, depending on the domain size and resolution, they can be very demanding from a computational viewpoint. Furthermore, training for modelers requires a high technical and scientific background and model calibration and validation is difficult to assess (Mearns, 2001).

As an alternative to dynamic models, statistical downscaling models have been developed. They are based on the view that regional climate is mostly a result of the large scale climatic state and regional/local physiographic features, e.g. topography, land-sea distribution and land use (Wilby, 2004). Statistical downscaling methods are generally classified in three groups: (i) regression models; (ii) weather pattern classification schemes and (iii) weather time series generators. A major advantage of these techniques in comparison with dynamical models is that they are computationally less demanding, and can be easily applied to the output of various GCMs scenarios, enabling a more accurate assessment of future uncertainties. The major theoretical limitation of statistical downscaling is that their basic assumption is not verifiable, i.e., the statistical relationships developed for the present day climate will also hold for the different forcing conditions in the future climates (Fowler, 2007).

The aim of this work was to assess the use of statistical downscaling methods to model precipitation extremes, focusing on urban areas, where this kind of events can cause floods. The outputs will integrate a risk assessment on floods for several Portuguese cities, with the quantification of the impacts of climate change on flood frequency and consequently on damage.

2 Methods

2.1 Tools and datasets

The chosen statistical downscaling approach is a hybrid between a stochastic weather generator and transfer function methods. Large-scale circulation patterns and atmospheric moisture variables are used to condition local scale weather parameters such as precipitation occurrence and intensity. Stochastic techniques are then used to artificially inflate the variance of the downscaled daily time series. This method was applied using the SDSM (**S**tatistical **D**own**S**caling **M**odel) tool version 4.2, developed by Wilby, Dowson and Barrow, 2001.

Daily precipitation, for Lisbon between 1961 and 2001, was obtained at the European Climate Assessment & Dataset (ECA&D) for the following meteorological station: **Name:** 177 LISBOA GEOFISICA; **WMO:** 08535; **Latitude:** 38º43' N; **Longitude:** 09º09' W; **Height:** 77m. For Coimbra the data was published by Valente, et al, 2008 for the **station Name:** COIMBRA GEOFISICA; **Latitude:** 40º 12' 25''; **Longitude:** 8º 25.4' W; **Height:** 140 m.

The chosen GCM was the coupled atmosphere-ocean HadCM3 developed by the Hadley Centre, with a horizontal resolution of 2.5º of latitude and 3.75º of longitude, with a global grid of 96 x 73 grid cells.

The HadCM3 daily predictors for the A2 and B2 scenarios were acquired at the Canadian Climate Change Scenarios Network (CCCSN). These predictors can also be downloaded from the National Center for Environmental Prediction NCEP/NCAR reanalysis project web site (http://www.cdc.noaa.gov/cdc/data.ncep.reanalysis.html) but for this particular study these datasets had to be interpolated to the same grid as the HadCM3 GCM (2.5º latitude x 3.75º longitude) and then normalized over the complete 1961-1990 period.

2.2 Exploratory analysis

The first step of the exploratory analysis was to look at the behavior of extreme precipitation between 1961 and 2001 by analyzing the number of days above the 99th percentile per year and the inter-annual variability of the 24 hour maximum per year. In the second step, daily maximum precipitation values per year where ranked and fitted to several probability density functions to choose the most appropriate and then calculate the different probability of non-exceedance/return periods which is an estimate of the likelihood of an flood event to occur.

The chosen probability density function was the Gumbel's Extreme Value Type I method, usually called EV I (Gumbel, E.J. 1954). The cumulative density function of the Gumbel method is the double exponential has showed in *Eq. 2.1*:

$$Eq.\ 2.2.1 \qquad F(x) = e^{-e^{-y}}$$

in which *F(x)* is the probability of non-exceedance. This way the probability of exceedance is the complementary probability to *F(x)*:

$$Eq.\ 2.2.2 \qquad G(x) = 1 - F(x)$$

The return period *T is the reciprocal of the probability of exceedance, therefore,*

Eq. 2.2.3 $$\frac{1}{T} = 1 - e^{-e^{-y}}$$

From Eq. 2.2.3 we have:

Eq. 2.2.4 $$y = -\ln \ln \frac{T}{T-1}$$

In the Gumbel method the precipitation are obtained from the frequency formula, *Eq.* 2.2.5:

Eq. 2.2.5 $$x = \bar{x} + Ks$$

where *s* is the standard deviation and $\bar{x}$ the mean of the population. The frequency factor *K* is evaluated with the frequency formula:

Eq. 2.2.6 $$y = \bar{y}_n + K\sigma_n$$

where σ_n is the standard deviation and $\bar{y}$ is the mean of the Gumbel distribution. These values are a function of record length *n*. From *Eq.* 2.2.5 and 2.2.6 we have:

Eq. 2.2.7 $$x = \bar{x} + \frac{y-\bar{y}}{\sigma_n} s$$

and finally with *Eq.* 2.2.4 we have the precipitation for a given return period.

Eq. 2.2.8 $$x = \bar{x} - \frac{\ln ln \frac{T}{T-1} + \bar{y}_n}{\sigma_n} s$$

2.3 Climate scenarios

SDSM condenses the task of statistically downscaling into five main steps: (i) data quality control and transformation; (ii) screening of predictor variables; (iii) model calibration and selection; (iv) model validation; and (v) scenario generation from GCM predictors.

The appropriate variables where chosen using the NCEP (National Center for Environmental Prediction) reanalysis predictors by calculating and analyzing the monthly correlations, the histogram of the residuals, the residuals versus the predicted variable and calculating the Durbin-Watson statistics which is a statistical test used to detect the presence of autocorrelation in the residuals.

The selected GCM grid cells for Lisbon and Coimbra downscaling models where different. Lisbon is closer to the Atlantic Ocean in the lower left vertex of HadCM3 grid cell 95x 21y, but after testing different combinations of predictors from different adjacent grid cells the 94x 21y cell was chosen. For Coimbra the HadCM3 95x 21y grid cell was chosen since the city is located near its center.

The HadCM3 A2 and B2 SRES scenarios were used to produce a synthetic dataset of daily precipitation from 1961 to 2099 and an analysis of extremes was conducted to represent the 2020s, 2050s and 2080s magnitudes of daily rainfall events (called return levels) for the 2, 5, 10, 20, 50 and 100 year return periods.

The predictors chosen for Lisbon and Coimbra are presented in Table 2..

Table 2.3.1 – List of predictors chosen for downscaling precipitation

Lisbon	*Coimbra*
Surface zonal velocity	*Surface vorticity*
Surface vorticity	*Surface wind direction*
850 hPa zonal velocity	*500 hPa zonal velocity*
Surface wind direction	*500 hPa geopotential height*
850 hPa air flow strength	*850 hPa airflow strength*
850 hPa meridional velocity	*Surface specific humidity*
850 hPa geopotential height	
Relative humidity at 850 hPa	
Near surface relative humidity	

In order to have a better representation of the extremes a fourth root transformation was applied to the predictor and a variance inflation and bias correction methods were integrated in the model.

To assess the relative change between the present return periods and the future climate scenarios the following steps were taken:

1. Calculation of current (1961-2001) return levels of all rainfall events with return periods between 1.05 and 900 years rainfall data using extreme value analysis (EV Type I).
2. Identification of the current return levels for 6 return periods (2 in 5, 10, 20, 50 and 100 year events) from step 1.
3. Step 1 was repeated using climate model data for the period 1961-2001 (control period), 2010-2039 (2020s), 2040-2069 (2050s) and 2070-2099 (2080s) and the scenarios A2 and B2.
4. For all time periods and scenarios it was calculated the climate scaling factors by making the difference between the precipitation model of the control period and the scenarios.
5. Results from step 4 were added to all return levels of the distribution function of the observations.
6. Identification of which future return periods have the closest return levels to those identified in step 2.

3 Results and Discussion

3.1 Exploratory data analysis

The exploratory data analysis aims to provide general information about extreme precipitation events connected with floods. Lisbon and Coimbra are urban areas with high population density and construction. In these areas, flood events usually occur due to heavy rain in short periods of time causing losses in goods and building structures.

3.1.1 Lisbon

The 24 hours maximum precipitation per year in Lisbon was used to adjust a probability density function that reflects the probability of non-exceedance of a given precipitation. Figure 3.1.1 shows the inter-annual variability of maximum precipitation between 1961 and 2001 while figure 3.1.2 explores the number of events above the 99th percentile as an indicator of the annual frequency of extreme precipitation for the same period.

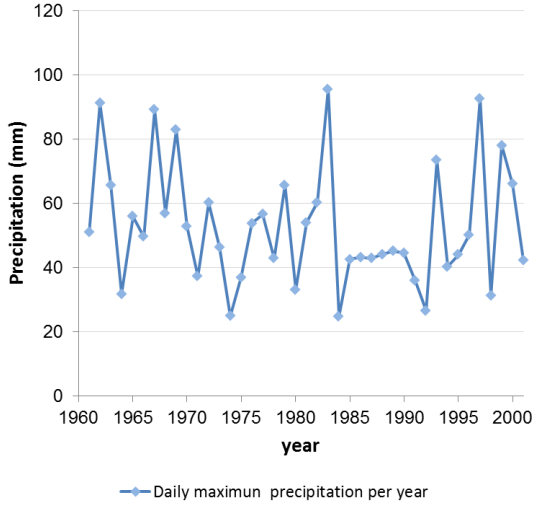

Fig. 3.1.1 – Maximum annual precipitation (mm) between 1961 and 2001 for Lisbon Geofísica meteorological station.

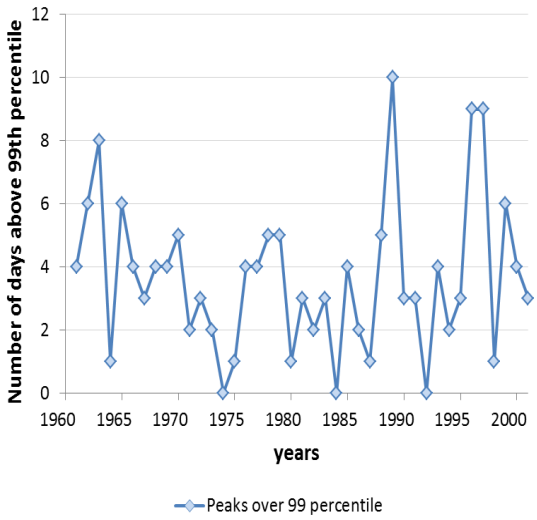

Fig. 3.1.2 – Number of days above the 99th percentile between 1961 and 2001 for Lisbon Geofísica meteorological station.

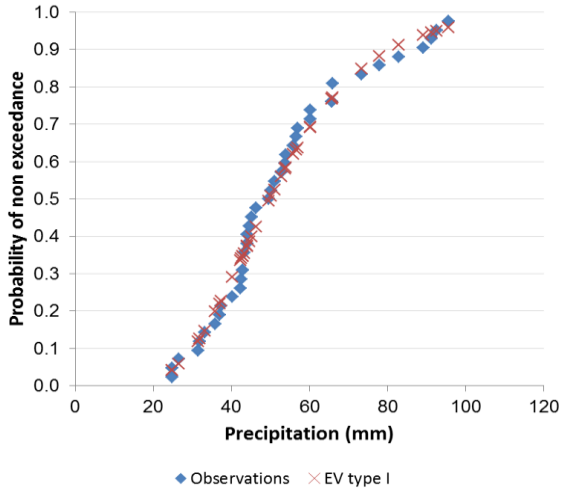

Fig. 3.1.3 – Comparison of the Gumbel's Extreme Value Type I density function and the ranking of the annual precipitation in Lisbon.

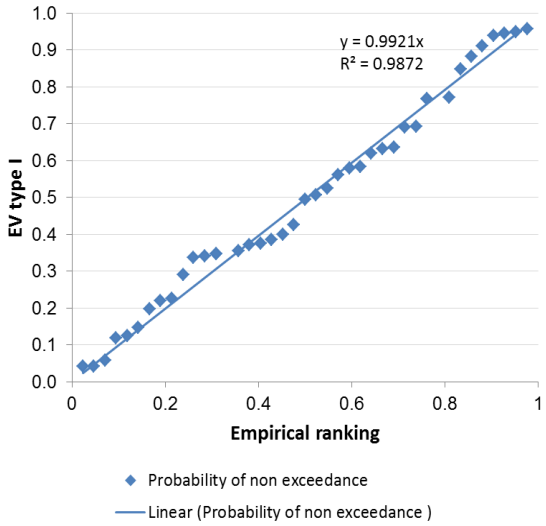

Fig. 3.1.4 – Linear fit between Gumbel's Extreme Value Type I density function and the precipitation ranking.

As showed in figure 3.1.3 and 3.1.4 the fit of the Gumbel's Extreme Value Type I function has coefficient of determination (R^2) close to one, attesting to the good fit between observations and model estimations. Table 3.1.1 shows the calculated Gumbel parameters used in equation 2.2.3, where σ and ȳ is given by the Gumbel's table showed in Appendices I.

Table 3.1.1 – Average and standard deviation of the Gumbel's table and the daily maximum precipitation per year between 1961 and 2001 for Lisbon.

Variable name	Value
standard deviation of the Gumbel distribution (σ)	0.5442
average of the Gumbel distribution (ȳ)	1.1436
sample average (μ)	52.76
standard deviation of the sample (*s*)	18.81

With the above parameters and taking into account Eq.2.2.3, the calculation of the return period for a given precipitation is given by the equation:

$$RP=-((EXP(EXP((1.1436*(52.76-x))/18.81-0.5442))/(1-(EXP(EXP((1.1436*(52.76-x))/18.81-0.5442))))))$$

where x is the precipitation in mm and *RP* is the return period in years.

The calculation of the return level (RL) for a given return period is done using the following expression:

$$RL=52.76+(((-LN(LN(RP/(RP-1))))-0.5442)/1.1436)*18.81$$

3.1.2 *Coimbra*

When comparing the results (Figure 3.1.2.2) from Coimbra with the one from Lisbon we can clearly see that the number of days per year above the 99th percentile is generally lower in Coimbra.

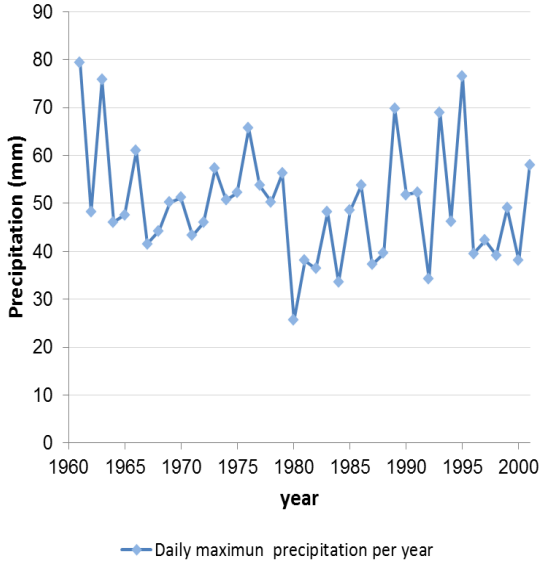

Fig. 3.1.2.1 - Maximum annual precipitation (mm) between 1961 and 2001 for Coimbra Geofísica meteorological station.

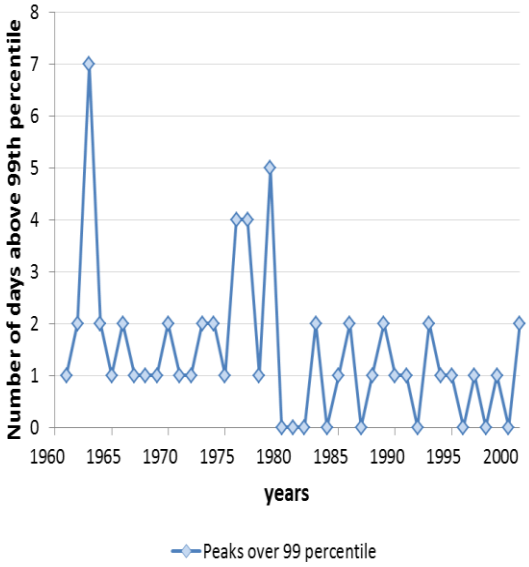

Fig. 3.1.2.2 - Number of days above the 99th percentile between 1961 and 2001 for Coimbra Geofísica meteorological station.

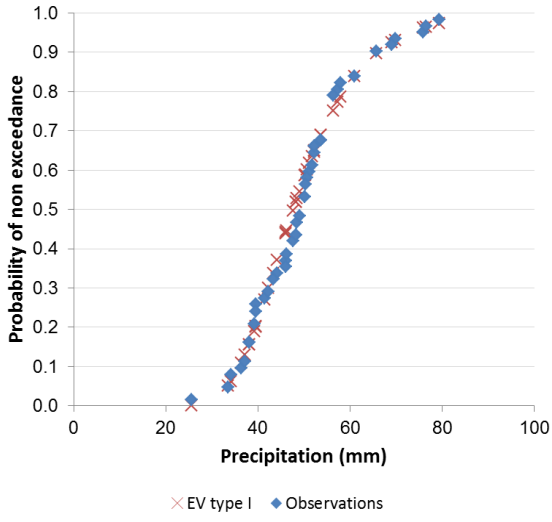

Fig. 3.1.2.3 - Comparison of the Gumbel's Extreme Value Type I density function and the ranking of the annual precipitation in Coimbra

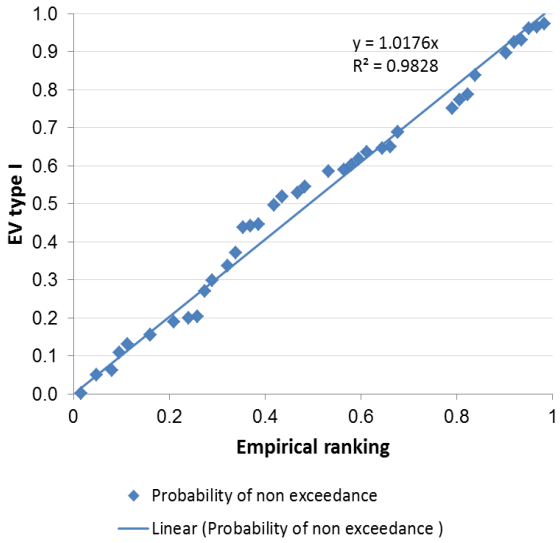

Fig. 3.1.2.4 - Linear fit between Gumbel's Extreme Value Type I density function and the precipitation ranking.

As showed in Figure 3.1.2.3 the adjustment between the probabilities of non-exceedance of the EV type I distribution and the empirical ranking of the observations is very good, as

proven by the coefficient of determination of ≈0.98 showed in figure 3.1.2.4. Table 3.1.2.1 shows the parameters used to adjust the observations to a EV type I distribution.

Table 3.1.2.1 – Average and standard deviation of the Gumbel's table and of the daily maximum precipitation per year between 1961 and 2001 for Coimbra.

standard deviation of the Gumbel distribution (σ)	0.5442
average of the Gumbel distribution (ȳ)	1.1436
sample average (μ)	49.93
standard deviation of the sample (*s*)	12.15

With the above parameters and taking into account Eq.2.2.3, the equation to calculate the return period for a given precipitation is:

$$RP=-((EXP(EXP((1.1436*(49.93-x))/12.15-0.5442))/(1-(EXP(EXP((1.1436*(49.93-x))/12.15-0.5442))))))$$

and the calculation of the return level for a given return period in Microsoft Excel is:

$$RL=49.93+(((-LN(LN(RP/(RP-1))))-0.5442)/1.1436)*12.15$$

3.2 Climate scenarios

3.2.1 Lisbon

The results for the downscaled 24 hour maximum precipitation per year for the reference period can be analyzed in figure 3.2.1.1 and table 3.2.1.1. The graphical comparison between the EV Type I of the observations and the EV Type I of the downscaled estimated values tell us that they are both very similar, but with a slight underestimation, meaning that the average and the standard deviation of the two samples are very close.

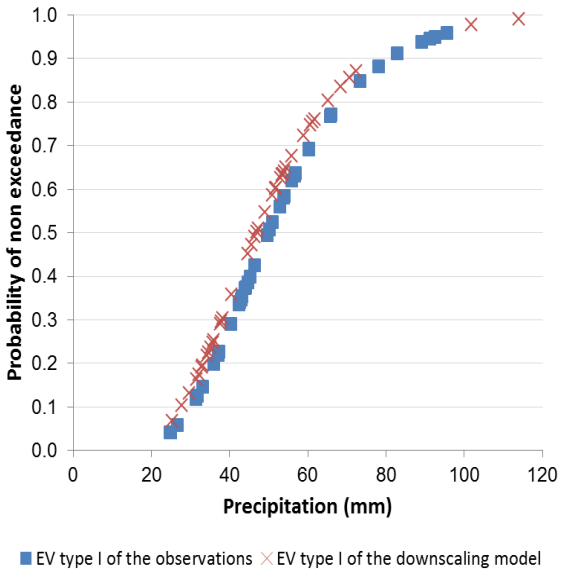

Fig. 3.2.1.1 - Comparison of the Gumbel's Extreme Value Type I density function of the observations and the downscaled model for Lisbon.

Gumbel RP (years)	Model PP (mm)	Obs. PP (mm)
1.05	23	25
5	65	68
10	77	81
15	84	88
20	88	93
30	95	99
40	100	104
50	103	108
60	106	111
80	111	116
100	114	119
500	140	146

Table 3.2.1.1 – Comparison between the Return Period (RP) of the downscaled precipitation (PP) model and the observations (Obs.).

Replacing the NCEP predictors with the HadCm3 A2 and B2 predictors gives us a picture on how precipitation projections tend to behave. Figure 3.2.1.2 shows the observed daily maximum precipitation per year between 1961 and 2001 and its projections between 2001 and 2099 indicating a possible slight decrease at the end of the XXI century. It is also important to notice the medium term variability of the precipitation that cyclically alternates from dry to wet periods. This cycle is clearer when analyzing river discharges and basin average precipitation rates. Recent studies show a relationship between this phenomena and the rate of change of the sun's orbital angular momentum, which is thought to modulate

the strength of the solar wind and sunspot dynamics under weak sunspot activity (Landscheidt, 2000).

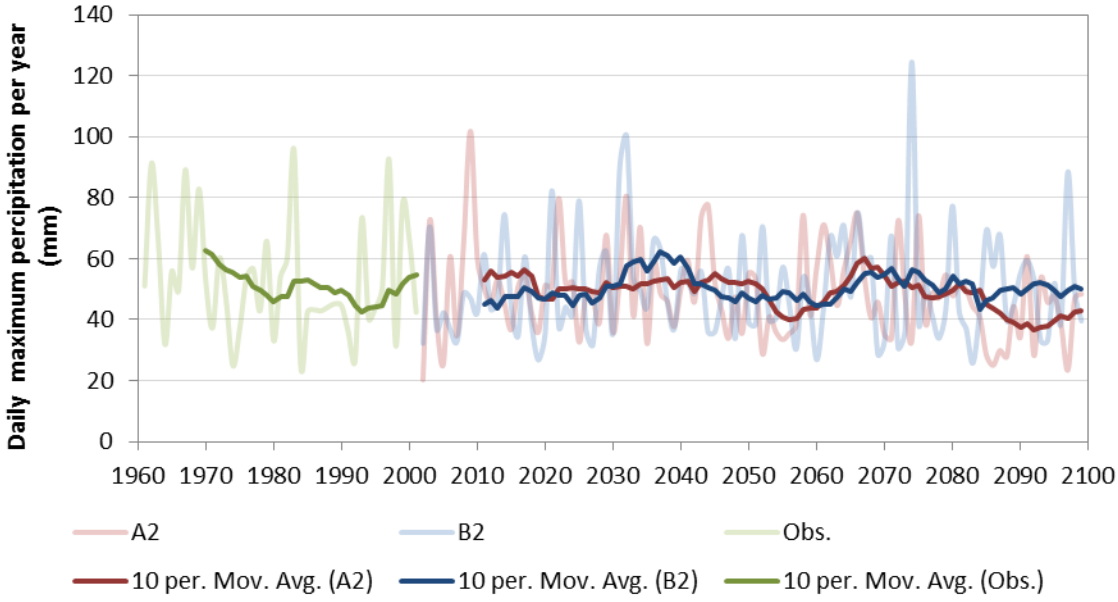

Fig. 3.2.1.2 – Observations (Obs.) and projections of the daily maximum precipitation per year in Lisbon for the HadCm3 A2 and B2 SRES in soft color lines and its 10 years moving averages in solid lines.

The projections of the 2, 5, 10, 20, 50 and 100 years return periods for the A2 and B2 scenario are respectively presented in figures from 3.2.1.3 to 3.2.1.8 and were calculated based on the five step procedure presented e 2.3. Each result was calculated with 30 years values, 2010-2039, 2040-2069 and 2070-2099, to represent the 2020's, 2050's and the 2080's periods, respectively. It is also important to mention that no homogeneity test was performed of the chosen time window, meaning that each result can be influenced by the dominant wet or dry cycle.

The overall results for Lisbon showed a high uncertainty regarding the definition of a signal trend. With the exception of the 2 year, both scenarios diverge regarding the evolution of the different return periods characterized by a slight decrease in return period in the B2 scenario for the 2020 and 2080 periods, where, inversely, the B2 scenario usually shows a stronger increase signal. Nevertheless, for 2050 period, both scenarios tend to agree on higher return periods when compared with the reference values. The two scenarios also present a greater uncertainty, given by a higher interval range between scenarios, at the end of the XXI century and for higher return periods.

Regarding the aforementioned two year return period, Figure 3.2.1.3 shows a slight decrease in both scenarios in the short (2020) and medium term (2050), meaning a tendency of higher frequencies of this level of precipitation. This tendency might have a significant impact on flood risk estimation in futures scenarios since it is well known that the two years return period precipitation in Lisbon is sufficient to trigger floods, leading to asset losses (Ana Lopes, et al, 2010).

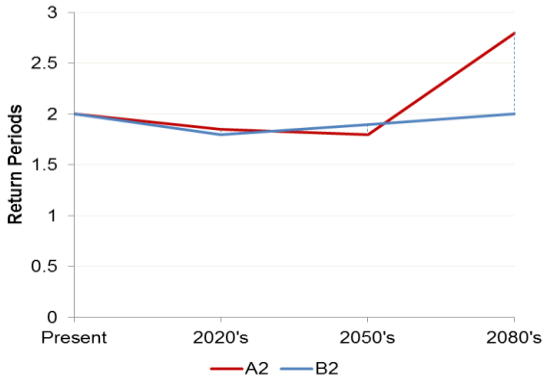

Fig. 3.2.1.3 – Short, medium and long term projections of the precipitation equivalent of the 2 years return period for the A2 and B2 scenario.

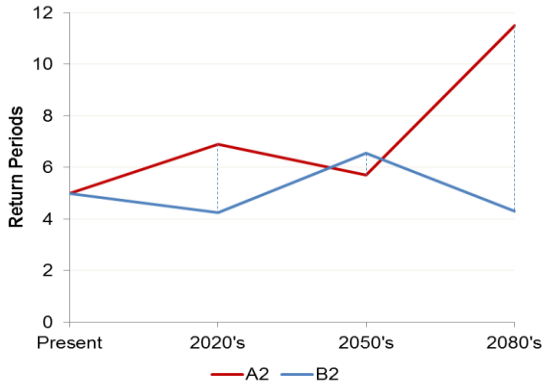

Fig. 3.2.1.4 - Short, medium and long term projections of the precipitation equivalent of the 5 years return period for the A2 and B2 scenario.

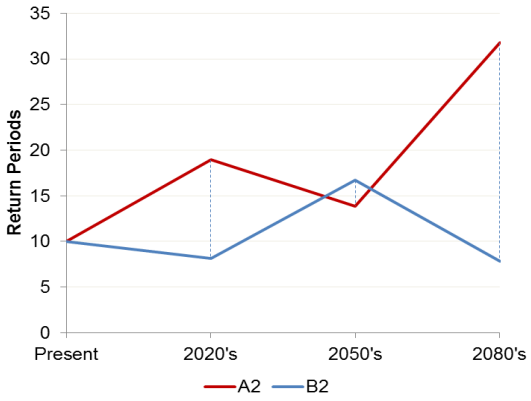

Fig. 3.2.1.5 - Short, medium and long term projections of the precipitation equivalent of the 10 years return period for the A2 and B2 scenario.

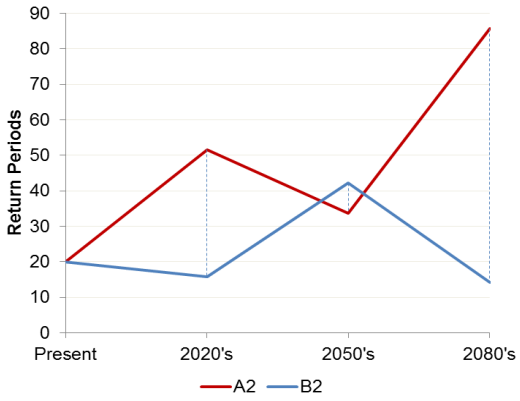

Fig. 3.2.1.6 - Short, medium and long term projections of the precipitation equivalent of the 20 years return period for the A2 and B2 scenario.

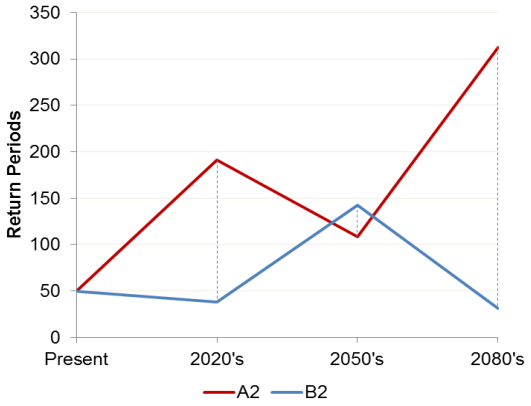

Fig. 3.2.1.7 - Short, medium and long term projections of the precipitation equivalent of the 50 years return period for the A2 and B2 scenario.

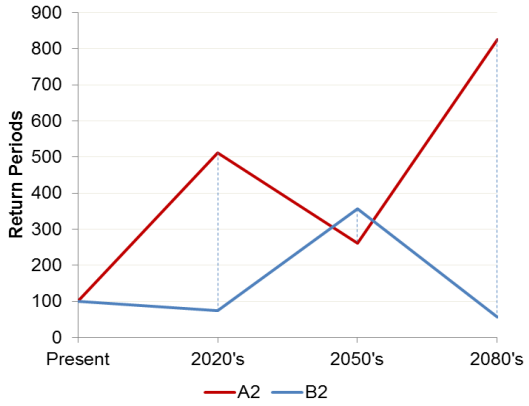

Fig. 3.2.1.8 - Short, medium and long term projections of the precipitation equivalent of the 100 years return period for the A2 and B2 scenario.

3.2.2 Coimbra

The same information presented for Lisbon is given in this section for Coimbra.

The analysis of figure 3.2.2.1 and table 3.2.2.1 also shows a good agreement between the EV I of the observations and the EV I of the downscaling precipitation results, but with minor overestimation of the precipitation for a given return period.

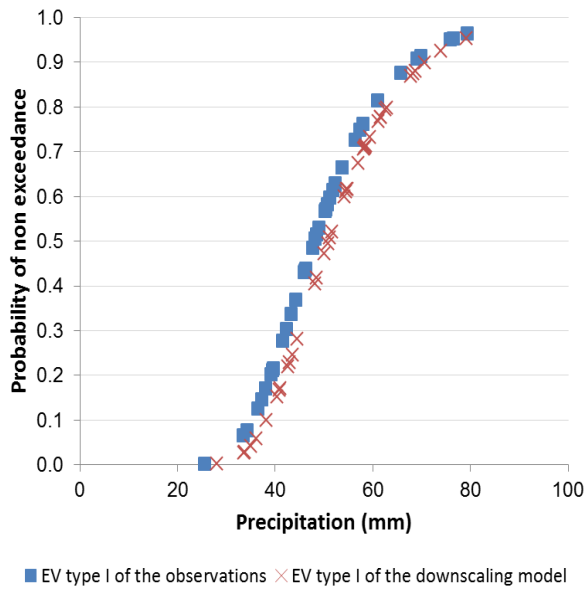

Fig. 3.2.2.1 - Comparison of the Gumbel's Extreme Value Type I density function of the observations and the downscaled model for Coimbra.

Return Period (years)	Model PP (mm)	Obs. PP (mm)
1.05	35	32
5	63	60
10	71	68
15	75	73
20	78	76
30	83	80
40	86	83
50	88	86
60	90	88
80	93	91
100	96	93
500	113	110

Table 3.2.2.1 - Comparison between the Return Period (RP) of the downscaled precipitation (PP) model and the observations (Obs.).

In figure 3.2.2.2 is also possible to identify the natural wet/dry cycle but the overall tendencies in both scenarios show an increase of 10 mm in the ten years moving average of the daily maximum precipitation values for the end of the XXI century, when compared with the reference period.

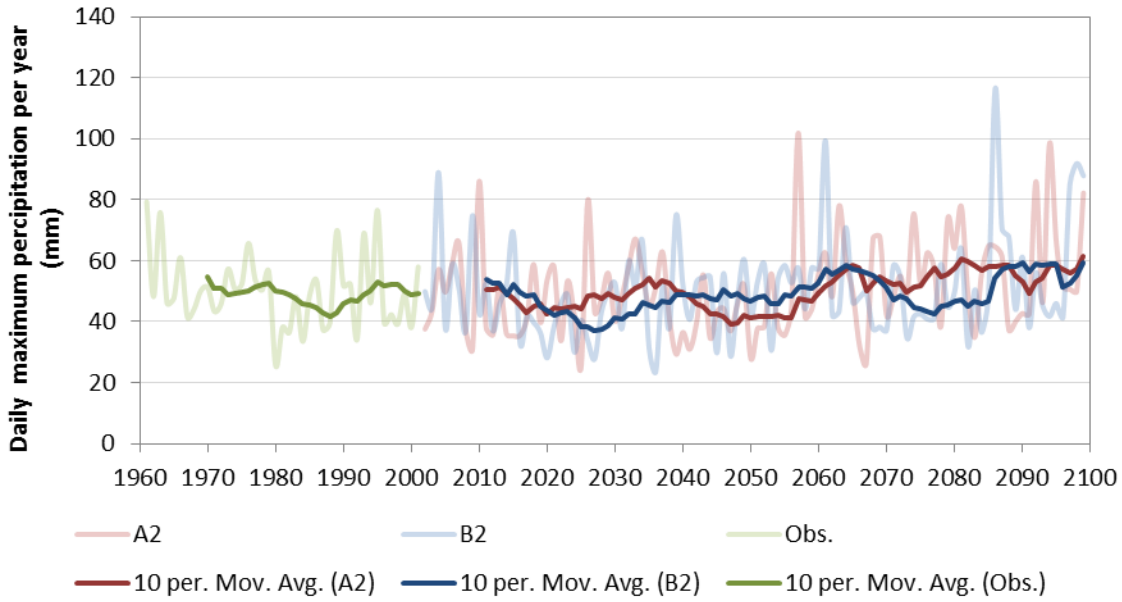

Fig. 3.2.2.2 – Observations (Obs.) and projections of the daily maximum precipitation per year in Coimbra for the HadCm3 A2 and B2 SRES in soft color lines and its 10 years moving averages in solid lines.

The analysis of the figures from 3.2.2.3 to 3.2.2.8 clearly show a convergence in both scenarios for a decrease in the return periods in the mid and end periods of the XXI century. With the exception of the 2 years return period, projections indicate that all the simulated precipitation events will likely become approximately twice as frequent by the end of the century.

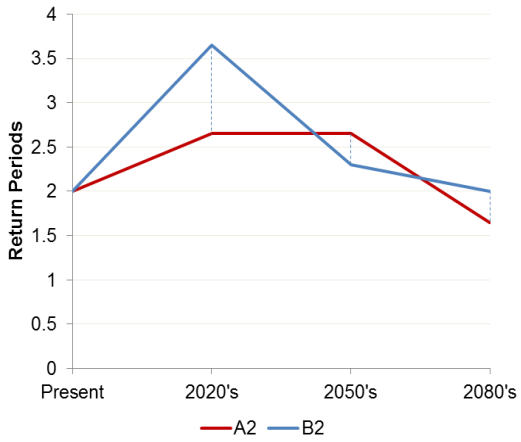

Fig. 3.2.2.3 - Short, medium and long term projections of the precipitation equivalent of the 50 years return period for the A2 and B2 scenario.

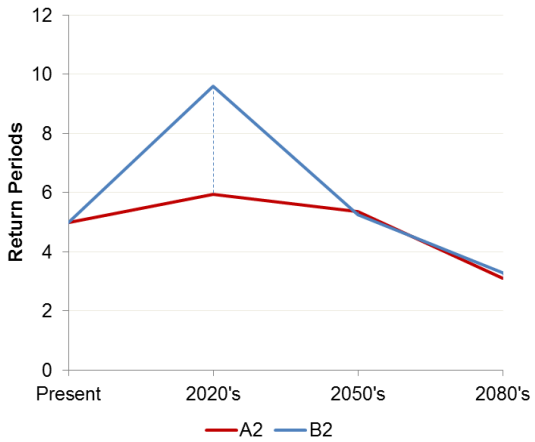

Fig. 3.2.2.4 - Short, medium and long term projections of the precipitation equivalent of the 50 years return period for the A2 and B2 scenario.

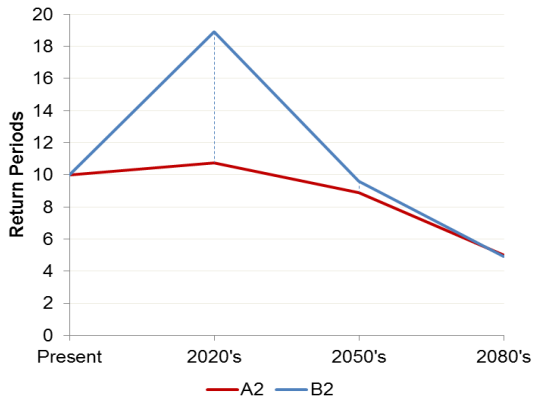

Fig. 3.2.2.5 - Short, medium and long term projections of the precipitation equivalent of the 50 years return period for the A2 and B2 scenario.

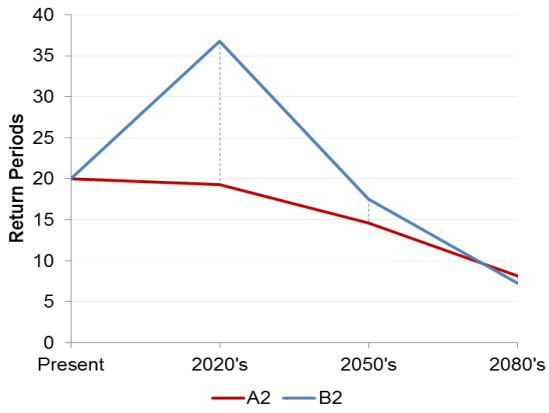

Fig. 3.2.2.6 - Short, medium and long term projections of the precipitation equivalent of the 50 years return period for the A2 and B2 scenario.

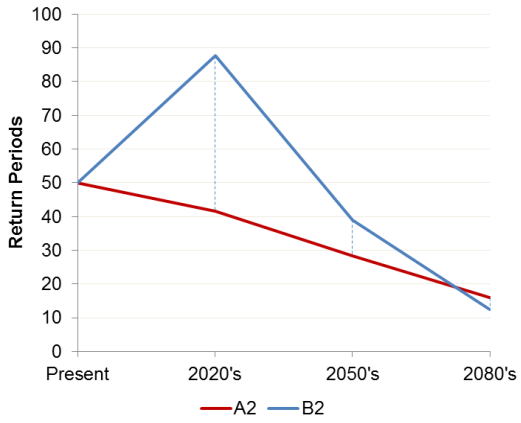

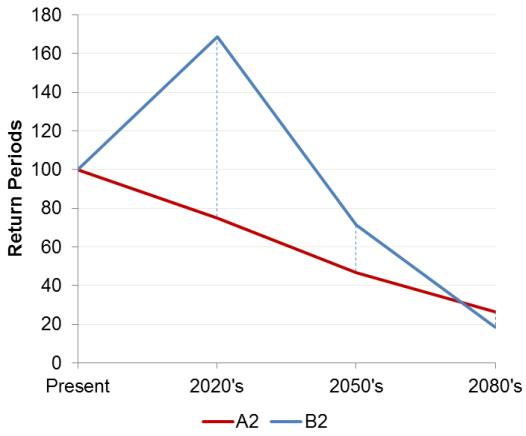

Fig. 3.2.2.7 - Short, medium and long term projections of the precipitation equivalent of the 50 years return period for the A2 and B2 scenario.

Fig. 3.2.2.8 - Short, medium and long term projections of the precipitation equivalent of the 50 years return period for the A2 and B2 scenario.

4 CONCLUSION

Regionalization of climate scenarios is an important procedure to access local climate variability that global climate models cannot represent due to their spatial resolution. Both statistical and dynamical downscaling techniques are often used to bridge the gap between the large and small spatial scale but both methods usually have difficulties representing precipitation extremes. This work showed that statistical methods can be used for downscaling extreme precipitation events but special attention should be given to: the GCM grid cell selection process; b) the selection of the predictors and; c) the integration of a variance inflation and bias correction methods. These three important steps are essential to improve model estimation, specially the last one, since it allows a better representation of precipitation extremes.

Results showed that the Gumbel's Extreme Value Type I probability distribution provided the best fit with the daily maximum precipitation per year values, with a coefficient of determination higher than 98% in Coimbra and Lisbon.

Overall results for Lisbon show a higher uncertainty in the definition of a signal trend for most of the return periods, although a slight tendency for a decrease in frequency is observed, with the exception of the 2 year return period. In the case of Coimbra results show a convergence in both scenarios towards a significant decrease in the return periods for the mid and end of the XXI century. This difference in behavior between the two locations might be partially explained by the relative geographical location of both cities. Portugal is located in a transitional climatic region between an Atlantic influenced temperate northern region and a more Mediterranean driven semi-arid region southern region. The SREX report (IPCC, 2012) shows a clearer increase in the frequency of extreme precipitations events for the first region, while results for the second are less pronounced and more uncertain. Since the Tagus basin, where Lisbon is located, corresponds to the transitional area between these two climatic regions, the extreme precipitation trend signal provides ambiguous interpretations, while Coimbra, more to the north, displays a stronger signal pointing towards an increase in the frequency of extreme precipitation events.

The recent Representative Concentration Pathways (RCP) are the latest generation of radiative forcing scenarios that provide input to climate models. For future work this analysis should include an ensemble of global climate models using these new RCPs for better estimation of extreme precipitation and representation of the uncertainties.

5 REFERENCES

Fowler HJ, Blenkinsop S, Tebaldi C (2007) Linking climate change modelling to impacts studies: recent advances in downscaling techniques for hydrological modelling. International Journal of Climatology 27:1547-1578

Gumbel, E.J. 1954. "Statistical theory of extreme values and some practical applications". Applied Mathematics Series, 33. U.S. Department of Commerce, National Bureau of Standards

IPCC (2012): Managing the Risks of Extreme Events and Disasters to Advance Climate Change Adaptation. A Special Report of Working Groups I and II of the Intergovernmental

Panel on Climate Change [Field, C.B., V. Barros, T.F. Stocker, D. Qin, D.J. Dokken, K.L. Ebi, M.D. Mastrandrea, K.J. Mach, G.-K. Plattner, S.K. Allen, M. Tignor, and P.M. Midgley (eds.)]. Cambridge University Press, Cambridge, UK, and New York, NY, USA, 582 pp.

Mearns, C. Fu (2001) *Regional Climate Information – Evaluation and Projections*. Chapter 10 in: Houghton, J. et al. (eds.). Climate Change 2001: The Scientific Basis. Intergovernmental Panel on Climate Change, Cambridge University Press, pp. 583-638.

Wilby RL, Dawson CW, Barrow EM (2002) SDSM - a decision support tool for the assessment of regional climate change impacts. Environmental Modelling & Software 17:147-159

Wilby RLC, S.P., Zorita E, Timbal B, Whetton P, Mearns L (2004) Guidelines for Use of Climate Scenarios Developed from Statistical Downscaling Methods.

Robert L. Wilby, and Christian W. Dawson (2007) SDSM 4.2 — A decision support tool for the assessment of regional climate change impacts.

Appendices I

Mean ȳ and Standard Deviation σ of Gumbel variate (y) versus record length (n)

n	$\bar{y}_n$	σ_n	n	$\bar{y}_n$	σ_n	n	$\bar{y}_n$	σ_n
8	0.4843	0.9043	35	0.5403	1.1285	64	0.5533	1.1793
9	0.4902	0.9288	36	0.5410	1.1313	66	0.5538	1.1814
10	0.4952	0.9497	37	0.5418	1.1339	68	0.5543	1.1834
11	0.4996	0.9676	38	0.5424	1.1363	70	0.5548	1.1854
12	0.5035	0.9833	39	0.5430	1.1388	72	0.5552	1.1873
13	0.5070	0.9972	40	0.5436	1.1413	74	0.5557	1.1890
14	0.5100	1.0095	41	0.5442	1.1436	76	0.5561	1.1906
15	0.5128	1.0206	42	0.5448	1.1458	78	0.5565	1.1923
16	0.5157	1.0316	43	0.5453	1.1480	80	0.5569	1.1938
17	0.5181	1.0411	44	0.5458	1.1499	82	0.5572	1.1953
18	0.5202	1.0493	45	0.5463	1.1519	84	0.5576	1.1967
19	0.5220	1.0566	46	0.5468	1.1538	86	0.5580	1.1980
20	0.5236	1.0628	47	0.5473	1.1557	88	0.5583	1.1994
21	0.5252	1.0696	48	0.5477	1.1574	90	0.5586	1.2007
22	0.5268	1.0754	49	0.5481	1.1590	92	0.5589	1.2020
23	0.5283	1.0811	50	0.5485	1.1607	94	0.5592	1.2032
24	0.5296	1.0864	51	0.5489	1.1623	96	0.5595	1.2044
25	0.5309	1.0915	52	0.5493	1.1638	98	0.5598	1.2055
26	0.5320	1.0961	53	0.5497	1.1653	100	0.5600	1.2065
27	0.5332	1.1004	54	0.5501	1.1667	150	0.5646	1.2253
28	0.5343	1.1047	55	0.5504	1.1681	200	0.5672	1.2360
29	0.5353	1.1086	56	0.5508	1.1696	250	0.5688	1.2429
30	0.5362	1.1124	57	0.5511	1.1708	300	0.5699	1.2479
31	0.5371	1.1159	58	0.5515	1.1721	400	0.5714	1.2545
32	0.5380	1.1193	59	0.5518	1.1734	500	0.5724	1.2588
33	0.5388	1.1226	60	0.5521	1.1747	750	0.5738	1.2651
34	0.5396	1.1255	62	0.5527	1.1770	1000	0.5745	1.2685

Source: Gumbel, E. J. (1958). *Statistics of Extremes.* Irvington, New York: Columbia University Press.